ELECTRONIC SUPPLEMENTARY INFORMATION (ESI)

I. Comparison between rheological data obtained by using the shear rate sweep and frequency sweep modes

All the viscosity data presented in the main text were obtained by using the shear rate sweep mode. We had also used the frequency sweep (or oscillatory) mode to crosscheck some data. Before discussing the crosscheck result, we describe each measurement mode in detail and display some representative data.

In the shear rate sweep mode, the shear rate $\dot{\gamma}$ was increased at constant logarithmic steps from 10^{-3} to 10 s^{-1}. In our setting, $\Delta[\log(\dot{\gamma})] = 0.125$. Upon each increment in $\dot{\gamma}$, the shear stress was measured. To ensure that the sample was in the steady flow state when the measurement was taken, the shear stress was assessed every 10 s. The steady state was reckoned when the shear stress value agreed within 5 % in three consecutive readings. The viscosity was then calculated to be the ratio of the steady-state shear stress divided by the applied shear rate. Figures S1(a) to (c) depict three representative sets of viscosity versus time data taken during the same shear rate sweep run on a PS425K-13nm-g5K PNC. Figures S1(a) and (b) were acquired as the shear rate was increased from 0 to 9.954×10^{-4} s^{-1} and 7.494×10^{-3} to 0.0100 s^{-1}, respectively (n.b. both 9.954×10^{-4} and 0.01 s^{-1} are below the dynamic crossover between the liquid and solid states according to the viscosity versus shear rate plot, which can be found further below in Figure S4(a)). For comparison, we also show in Figure S1(c) the data acquired as the shear rate was increased from 2.373 to 3.164 s^{-1} (above the crossover). In Figures S1(a) and (b), the viscosity rises monotonically and stabilizes toward a steady-state value before the end of the plot. Moreover, the values found in the end of the two plots are the same. In contrast, the viscosity in

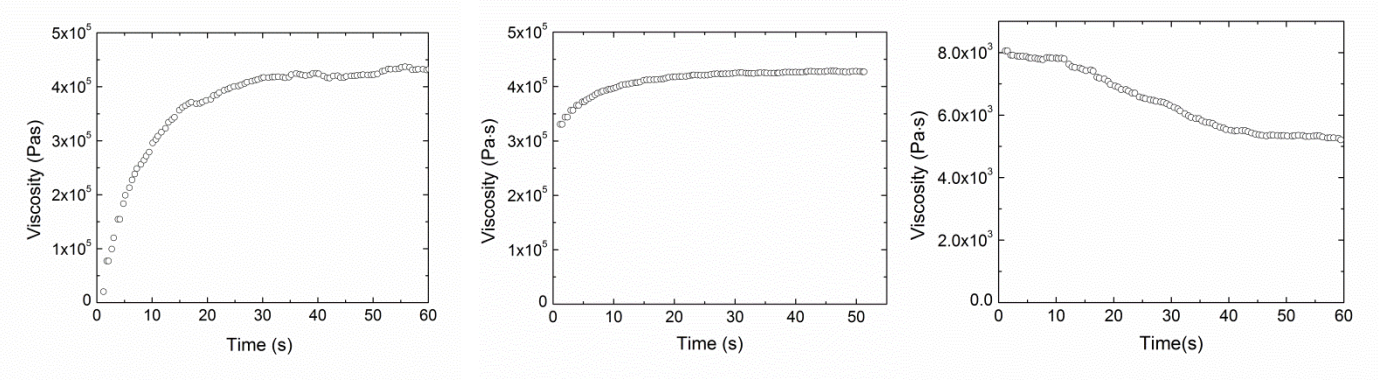

(a) (b) (c)

Fig. S1. Viscosity (≡ (shear stress)/(applied shear rate)) versus time acquired upon a shear rate jump from 0 to 9.954 $\times 10^{-4}$ s^{-1} (a), 7.494 $\times 10^{-3}$ to 0.0100 s^{-1} (b) and 2.373 to 3.164 s^{-1} (c). All three data were acquired in the same shear rate sweep run of PS425K-13nm-g-5K at 455 K.

Figure S1(c) decreases with time, indicating that the sample suffered shear thinning. These observations show that the sample viscosity, as determined to be the steady-state value taken from plots like those shown in Figure S1(a) and S1(b) at low shear rates below the dynamic crossover, were indeed acquired under the steady-flow condition. Moreover, the measurements were independent of the applied shear rate, consistent with requirement for zero-shear viscosity measurement.

In the frequency sweep mode, the angular frequency, ω, was varied from 0.1 to 10 rad/s as the storage and loss moduli, *G*' and *G*'', were measured. From the measurement, the complex viscosity, $|\eta^*| \equiv [(G')^2 + (G'')^2]^{1/2}/\omega$ was calculated. The zero-shear viscosity was taken to be the complex viscosity in the $\omega \rightarrow 0$ limit. Please note that in the $\omega \rightarrow 0$ limit, $G' \rightarrow 0$ and so $\lim_{\omega \to 0} |\eta^*| = \lim_{\omega \to 0} \left(G''/\omega \right)$, consistent with the usual relation used to determine zero-shear viscosity in oscillatory measurements. Besides the zero-shear viscosity, the elastic modulus, *G*, can also be determined by using the relation, $G = G'(\omega)\big|_{\tan\delta \to \min}$, where $\tan\delta \equiv G''/G'$. Figures S2(a) and 2(b)

show representative *G*' and *G*'' versus ω data obtained from a neat PS and a PNC sample, respectively. Figure S3(a) and 3(b) show the tan δ versus ω arising from these data. From these figures, one deduces that the minimum of tan δ occurs at ω = 316 and 251 rad/s for the neat and PNC sample, respectively. The *G*' value hence obtained is 2.0 and 2.3 × 10^5 Pa, respectively. Both values are in excellent agreement with the literature value. [1]

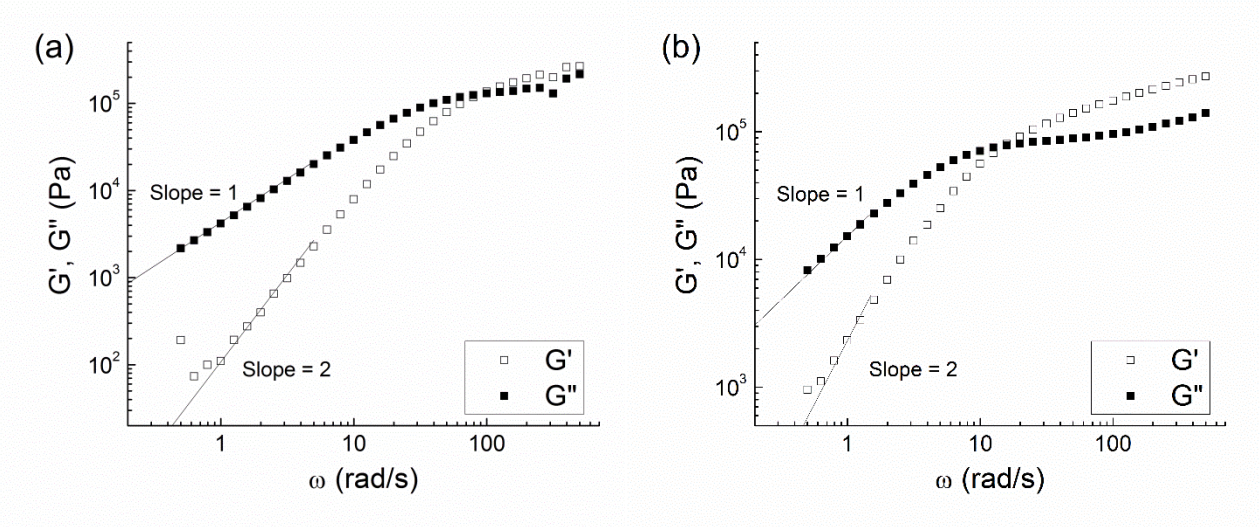

Fig. S2. Representative frequency sweep measurements obtained from a neat PS48K (a) and a PS139K+rc13nm-g-5.1K PNC (b) at 463 K.

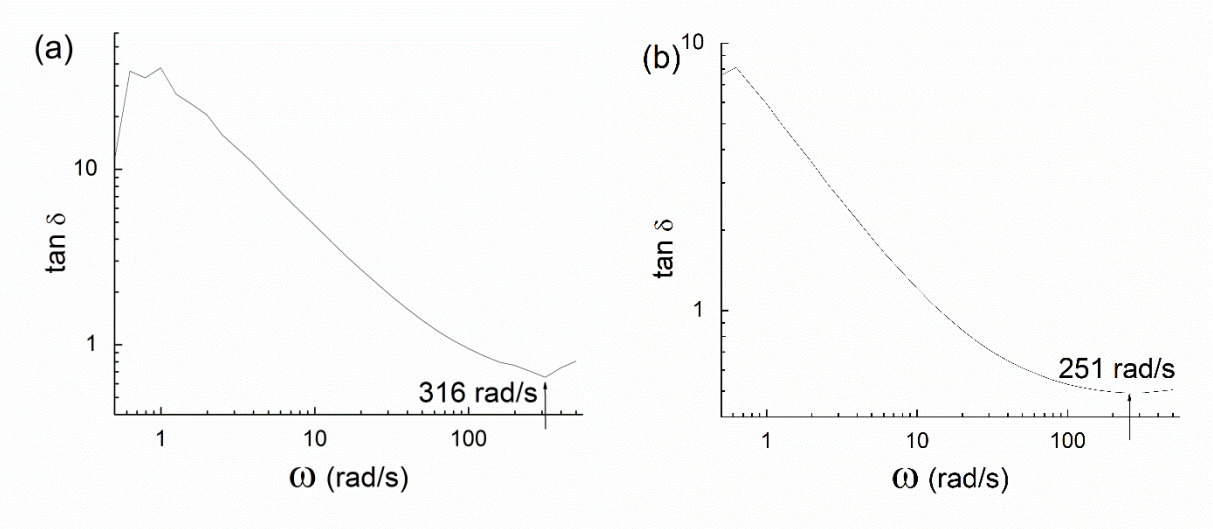

Fig. **S3.** tan δ versus ω deduced from the data of Figure S2(a) and S2(b), respectively.

Shown in Figure S4(a) and S4(b) are the viscosity measurements obtained by using the shear rate sweep and frequency sweep mode, respectively, from samples made of the same PNC material (PS425K+rc13nm-g,THF(precipitate)). The viscosities deduced from these data are shown in Table S1. As seen, the viscosity ratios obtained from the two measurement modes agree.

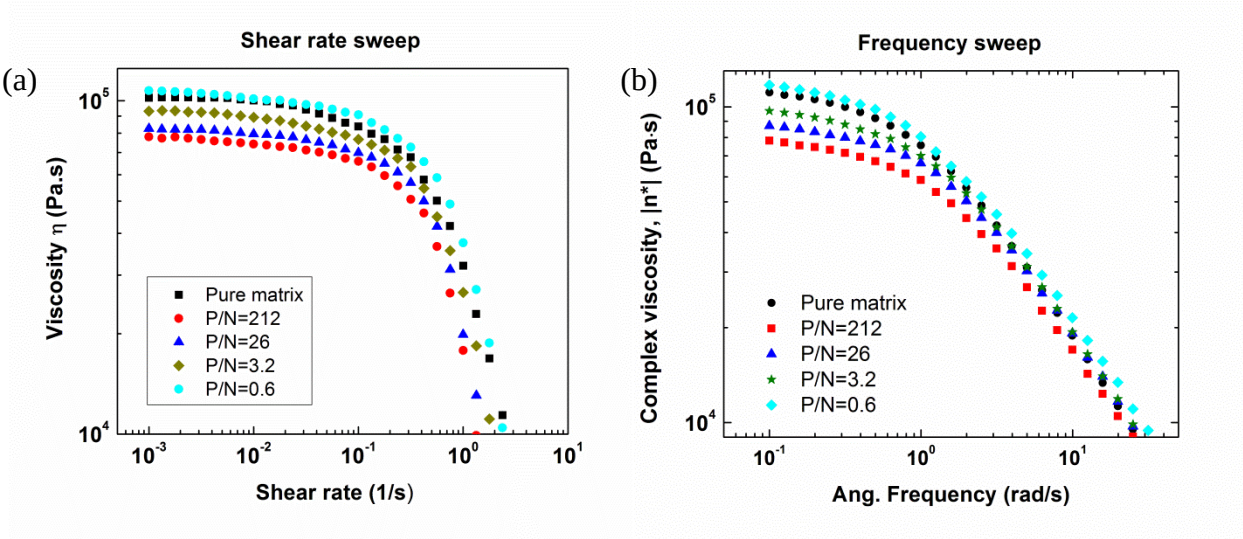

Fig. S4. (a) Viscosity, η, vs. shear rate and (b) complex viscosity, $|\eta^*|$, vs. angular frequency, ω, as calculated from the G' and G" vs. ω measurements of the PS425K+rc13nm-g,THF(precipitate) PNCs and their corresponding host polymer at 473 K. Before measurement, the samples were annealed at 423 K for 5 h.

Table S.1 Zero-shear viscosities and viscosity ratios deduced from Fig. S4.

Sample	η (Pa·s)	η/η_{host} (Pa·s)	Sample	η (Pa·s)	η/η_{host} (Pa·s)
P/N = 0.6	107300	1.05	P/N = 0.6	117150	1.15
P/N = 3.2	93000	0.91	P/N = 3.2	97050	0.95
P/N = 26	82500	0.81	P/N = 26	87100	0.85
P/N = 212	78000	0.76	P/N = 212	78160	0.77

II. Correlation between the Viscosity Ratio and Modulus Ratio and the Implication

Figure S5 shows the viscosity ratio versus elastic modulus ratio of six series of PNCs that had been briefly annealed for 5 h at 423 K. Details of the samples are given in Table S2. The measurement temperatures, also specified in Table S2, were chosen so that the frequency window spans the crossover between the viscous and elastic dynamic regimes.

The data of Figure S5 show that the sample viscosity correlates positively with the elastic modulus. Richter et al. [2] noted that the plateau modulus of PNCs usually follows $G'(\phi) = G'_{Host}(\phi) \times (1 + [\eta]\phi + \ldots)$, where ϕ is the nano-particle volume fraction and $[\eta]$ the intrinsic viscosity. Observing the relation that defines intrinsic viscosity, namely $\eta(\phi) = \eta_{Host}(1 + [\eta]\phi) + \ldots)$, then for very dilute composites, $G'(\phi) / G'_{Host}(\phi) = \eta(\phi) / \eta_{Host}$. This relation, also shown

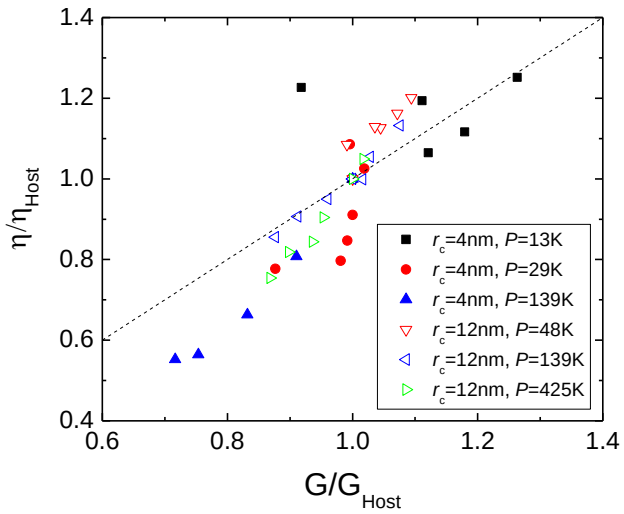

Figure S5. Viscosity ratio vs. elastic storage modulus ratio of the PNCs specified in Table S2. The dashed line indicates the relation $\eta/\eta_{Host} = G/G_{Host}$.

Table S.2 Sample Specifications for the Data shown in Fig. S5*

PNCs	P/N
PS13K+rc4nm-g	0.19
(T = 413 K)	0.25
	1.3
	2.5
	14
PS29K+rc4nm-g	0.41
(T = 433 K)	0.57
	2.9
	5.7
	15
	31
PS139K+rc4nm-g	2.0
(T = 463 K)	8.4
	27
	150

PNCs	P/N
PS48K+rc13nm-g	0.69
(T = 443 K)	2.9
	9.4
	24
	60
PS139K+rc13nm-g	0.21
(T = 463 K)	1.0
	2.0
	8.4
	27
	107
PS425K+rc13nm-g	0.63
(T = 473 K)	3.2
	8.3
	26
	83
	330

***** All samples were prepared by using THF as the solvent and the precipitation method for processing. Those containing the r_c = 4 nm nanoparticles are not discussed in the main text.

in Figure S5 (dashed line), is seen to account for the data roughly. Importantly, this result shows that the relaxation time of the dynamics, $\tau \approx \eta/G$, is similar between the PNCs and the corresponding host polymer. Therefore, the much slower relaxation seen of the sample viscosity (Figures 3-4 in the main text) should involve factors extrinsic to the polymer. Here, we propose it to be due to relaxation of the adsorbed chains on the NP and/or sample substrate surface.

III. Definitions and Procedures of Extracting $t_{equilibrium}$ and $\delta\eta_{fit}/\eta_{24h}$ from Experiment

Figure S6 shows the data of η/η_{24h} versus t (solid squares) from PS425K,THF(cast), with which we exemplify the definitions of $t_{\text{equilibrium}}$ and $\delta\eta_{\text{fit}}/\eta_{24h}$ and how they were determined from the data. The solid line is the best fit to the expression, $y = \eta_\infty/\eta_{24h} - (\eta_\infty/\eta_{24h} - \eta_0/\eta_{24h})\exp(-t/\tau)$, where η_∞/η_{24h}, η_0/η_{24h} and τ are fit parameters. Figure S6 shows that η_∞/η_{24h} and η_0/η_{24h} corresponds to the value of the fit function at $t = \infty$ and0, respectively. The characteristic time, $t_{\text{equilibrium}}$, is defined by $t_{\text{equilibrium}} \equiv -\tau \ln(0.1)$, namely the time for the fit function to rise by 90% of its maximum amount of change or $\frac{9}{10}\frac{(\eta_\infty - \eta_0)}{\eta_{24h}}$ from $t = 0$. We define the % change in η by $\delta\eta_{\text{fit}}/\eta_{24h} \equiv \eta_\infty/\eta_{24h} - \eta(t = 24\text{h})/\eta_{24h} = \eta_\infty/\eta_{24h} - 1$.

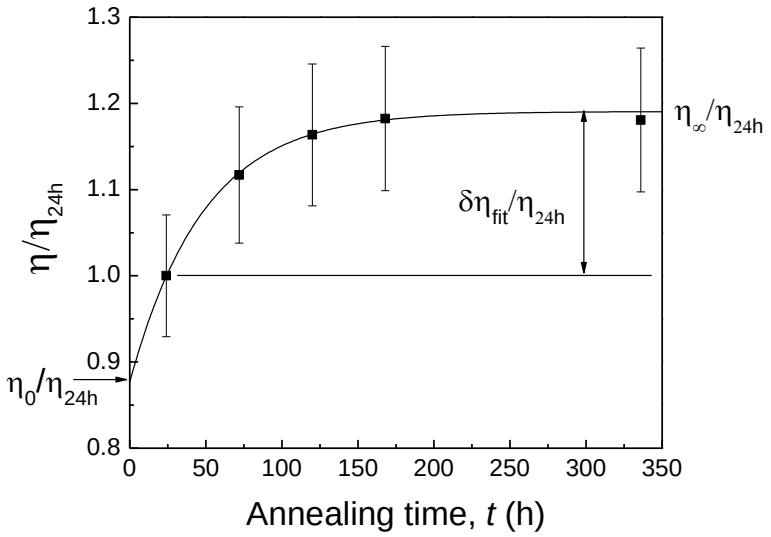

Figure S6. Illustration of how $\delta\eta_{\text{fit}}/\eta_{24h}$ of a sample is defined. The η/η_{24h} versus t of PS425K,THF(cast) (solid squares) is used for exemplification. The solid line is the best fit to the expression, $y = \eta_\infty/\eta_{24h} - (\eta_\infty/\eta_{24h} - \eta_0/\eta_{24h})\exp(-t/\tau)$, where η_∞/η_{24h}, η_0/η_{24h} and τ are fit parameters. The fit values of η_0/η_{24h}, η_∞/η_{24h} and $\delta\eta_{\text{fit}}/\eta_{24h} \equiv \eta_\infty/\eta_{24h} - 1$ are indicated in the figure.

References

1. S. Onogi, T. Masuda and K. Kitagawa, *Macromolecules*, 1970, **3**, 109-116.

2. K. Nusser, G. J. Schneider, W. Pyckhout-Hintzen and D. Richter, *Macromolecules*, 2011, **44**, 7820–7830.